Stage disorder of random-mixture graphite intercalation compounds

Stage disorder of random-mixture graphite intercalation compounds

Itsuko S Suzuki and Masatsugu Suzuki

Department of Physics and Materials Research Center, State University of New York at Binghamton, Binghamton, New York 13902-6000, USA

Abstract. The stage disorder of random mixture-GICs (RMGICs), stage 2 $Co_cM_{1-c}Cl_2$-GICs (M = Mn, Ni), has been studied by means of $(00L)$ x-ray diffraction. The $(00L)$ x-ray diffraction pattern shows the prominent feature that the stage-disorder induced peak shift and full-width at half-maximum of the Bragg reflections oscillate as a function of the Bragg index of stage 2. We present a model calculation of the $(00L)$ x-ray scattering intensity for systems with a stage disorder, which shows that the fractional probability of each stage is uniquely determined from the Bragg index dependence of the stage-disorder induced peak shift and full-width at half-maximum. The fractional probability of these compounds is determined by this method, and is discussed in terms of the scaling law relating the stage disorder to domain size (island size), charge transfer and temperature. The interlayer repulsion energy of these compounds which is the key for the stage order is shown to have the form of $u_i = v_0 i^{-\alpha}$ with $\alpha \approx 1$ and 1.8×10^{-3} eV $< v_0 < 1.8 \times 10^{-2}$ eV.

1. Introduction

Recently, stage disorder of graphite intercalation compounds (GICs) has received both experimental and theoretical interest (Kirczenow 1990). The staging structure of graphite intercalation compounds (GICs) is characterized by the stage number which refers to the number of graphite layers separating adjacent intercalate layers. Stage disorder is a random arrangement of packages with a different stage along the c-axis, where the package with stage i refers to an intercalate layer plus i graphite layers. The $(00L)$ x-ray diffraction pattern of GICs with stage disorder is characterized by (i) the full-width at half-maximum (FWHM) of the Bragg reflections, which depends on the index L, and (ii) the peak shift (PS) of the Bragg reflections from that of the pure stage, which depends on the index L. Fuerst et al (1983) have done the $(00L)$ x-ray diffraction of a donor K-GIC sample consisting of a random mixture of 76% stage 7 and 24% stage 8 packages, and have found that the peak shift of the Bragg reflections from its ideal stage 7 as a function of the index L shows an oscillatory behaviour. Hohlwein and Metz (1974) and Metz and Hohlwein (1975) have also found a characteristic stage disorder-induced broadening and peak shift of x-ray Bragg reflections for an acceptor $FeCl_3$-GIC.

Kirczenow (1985) has proposed a scaling law which provides a framework for understanding the stage disorder of donor and acceptor GICs. The scaling law indicates that the degree of stage disorder is related to (i) domain size in intercalate layers, (ii) charge transfer, (iii) filling factor and (iv) temperature. The in-plane order of the intercalate

layer is not related to stage disorder. The stage disorder is measured as the fraction of stage-i unit which is approximated by a Gaussian distribution with a peak at the dominant stage $\langle i \rangle$. The width of the Gaussian distribution

$$\sigma_{\langle i \rangle} = [(k_B T)/(N_0 x^2 (\partial^2 u_i/\partial i^2)_{i=\langle i \rangle})]^{1/2} = [(k_B T \langle i \rangle^{\alpha+2})/(N_0 x^2 v_0 \alpha(\alpha+1))]^{1/2} \qquad (1)$$

is a measure of stage disorder, where T is temperature, N_0 is domain size of the intercalate layer, i.e. the in-plane dimension of intercalate islands, x is the filling factor of domains, u_i is the interlayer repulsive interaction of the form $u_i = v_0 i^{-\alpha}$, where v_0 and α are constants. The scaling law indicates the importance of the repulsive interlayer interaction u_i. The degree of stage disorder increases as stage $\langle i \rangle$ and temperature increase and as domain size and filling factor decrease. The value of v_0 is a measure of charge transfer, so the degree of stage disorder increases as charge transfer decreases. The charge transfer of acceptor GICs is smaller than that of donor GICs. The intercalate layers of acceptor $CoCl_2$-GIC, $MnCl_2$-GIC and $NiCl_2$-GIC are known to be formed of small islands whose periphery provides an acceptor site for the charge transferred from the graphite layers. The size of these islands is much smaller than the domain size of donor GICs. The scaling law explains well the experimental evidence that the acceptor GICs exhibit more stage disorder than donor GICs.

Most experimental studies on the stage disorder have, until now, dealt with donor GICs such as alkali-metal GICs (Misenheimer and Zabel 1985, Kim *et al* 1986, Huster *et al* 1987, Cajipe *et al* 1989). In contrast to these compounds, there have been few systematic studies on the stage disorder of acceptor GICs. In this paper we report the experimental results of $(00L)$ x-ray diffraction on random mixture-GICs (RMGICs), stage 2 $Co_cM_{1-c}Cl_2$-GICs (M = Mn, Ni) in which two kinds of magnetic intercalants are distributed at random over the same intercalate layer (Yeh *et al* 1990, Suzuki *et al* 1991). These compounds are expected to provide a model system for studying the stage disorder of acceptor GICs. In these systems, the alternation between graphite and intercalate layers is no longer periodic and statistical analysis of the x-ray data is required to obtain a detailed microscopic description of the stacking sequence. We find from the $(00L)$ x-ray diffraction pattern of these compounds that the peak shift and full-width at half-maximum of the Bragg reflections oscillate as a function of the Bragg index. We present a model calculation of the $(00L)$ x-ray scattering intensity for $Co_cM_{1-c}Cl_2$-GICs with stage disorder. The model calculation shows that (i) the oscillation of a stage-disorder induced peak shift and full-width at half-maximum is one of the most noticeable features, and that (ii) the fractional probability of stage i can be determined from the Bragg index dependence of the stage-disorder induced peak shift and full-width at half-maximum. This method developed here is used to determine the fractional probability of stage 2 $Co_cM_{1-c}Cl_2$-GICs. Finally, the form of the interlayer repulsion energy of these compounds, which is responsible for stage order, will be discussed by applying the scaling law to experimental results of the fractional probability.

2. Model of stage disorder

2.1. Model calculation of x-ray scattering intensity with stage disorder

Here we present a simple model calculation of the $(00L)$ x-ray scattering intensity for $Co_cM_{1-c}Cl_2$-GICs (M = Mn, Ni) with a stage disorder, based on the theory first proposed by Hendricks and Teller (1942), and subsequently modified by Kakinoki and Komura
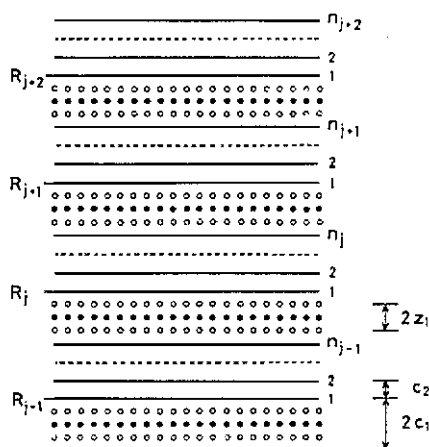
Figure 1. Model of the stage disorder along the c-axis for the $Co_cM_{1-c}Cl_2$-GICs (M = Mn, Ni): graphite layer (solid line), Co_cM_{1-c} layer (closed circle) and upper and lower Cl layers (open circle).

(1952). We assume that $Co_cM_{1-c}Cl_2$-GIC has a c-axis stacking sequence as shown in figure 1, where $2c_1$ is the distance between adjacent graphite layers with the gallery occupied by the $Co_cM_{1-c}Cl_2$ intercalate layer and c_2 is the distance between adjacent graphite layers without the intercalate layer. The jth $Co_cM_{1-c}Cl_2$ intercalate layer forms a three-layer structure where the Co_cM_{1-c} layer is sandwiched between upper and lower Cl layers and located at $r = R_j - c_1 (j = 1, 2, \ldots)$, and the distance between the Co_cM_{1-c} layer and the Cl layer is z_1. There are n_j graphite layers between the jth and $j + 1$th $Co_cM_{1-c}Cl_2$ intercalate layers. The jth $Co_cM_{1-c}Cl_2$ intercalate layer and the n_j graphite layers form the jth package with stage number n_j. The structure factor of the jth package with stage number n_j is

$$S_j(Q) = V_{n_j}(Q) \exp(iQR_j) \tag{2}$$

with

$$R_j = 2c_1 + \sum_{i=1}^{j-1} \{2c_1 + c_2(n_i - 1)\} \qquad R_1 = 2c_1 \tag{3}$$

and

$$V_{n_j}(Q) = \exp(-iQc_1)\{V_I(Q) + V_C(Q) \sum_{k=1}^{n_j} \exp iQ[c_1 + (k-1)c_2]\}. \tag{4}$$

Here, $V_C(Q)$ and $V_I(Q)$ are the structure factors of each graphite layer and intercalate layer respectively, and are expressed by

$$V_C(Q) = \rho_C b_C(Q) \tag{5}$$

and

$$V_I(Q) = \rho_{Co} b_{Co}(Q) + \rho_M b_M(Q) + 2\rho_{Cl} b_{Cl}(Q) \cos(z_1 Q) \tag{6}$$

where $b_i(Q)$ is the atomic form factor of the i-atom (i = Co, M, Cl and C), and ρ_i is the number of i-atoms per unit area. For the system consisting of the first package with stage number n_1, the second package with stage number $n_2, \ldots$, the jth package with stage

number n_j, and the Nth package with stage number n_N, we find the x-ray scattering intensity given by

$$I_N(Q) = \langle S(Q)S^*(Q)\rangle_{\text{av}} \tag{7}$$

where

$$S(Q) = \sum_{j=1}^{N} S_j(Q) \tag{8}$$

and $\langle\ldots\rangle_{\text{av}}$ denotes a configurational average expressed in terms of f_r and P_{sr} such that

$$\sum_r f_r = 1 \qquad \sum_s P_{sr} = 1 \qquad \sum_r P_{sr}f_r = f_s. \tag{9}$$

Here f_r is the probability of a package having stage r, and P_{sr} is the probability of a package, next to the package with stage r, having stage s. Note that $P_{sr} = f_s$ for a completely random distribution. The probability of the jth package having the stage r is obtained by

$$P_j(r) = \sum_{n_{j-1}} \sum_{n_{j-2}} \ldots \sum_{n_1} P_{rn_{j-1}} P_{n_{j-1}n_{j-2}} \ldots P_{n_2n_1} f_{n_1} = f_r. \tag{10}$$

Then the x-ray scattering intensity can be described as

$$I_N(Q) = N\,\text{Tr}(\mathbf{FV}) + \sum_{h=1}^{N-1} (N-h)\,\text{Tr}\{\mathbf{FV}(\mathbf{P\Phi})^h\} + \sum_{h=1}^{N-1} (N-h)\,\text{Tr}\{\mathbf{FV}^*(\mathbf{P\Phi}^*)^h\} \tag{11}$$

in terms of the matrices $\mathbf{V}$, $\mathbf{F}$, $\mathbf{P}$ and $\mathbf{\Phi}$ whose elements are defined by

$$(\mathbf{FV})_{rs} = f_r V_{rs} \qquad (\mathbf{P\Phi})_{rs} = P_{rs}\varphi_s \qquad (\mathbf{FV}^*)_{rs} = f_r V_{rs}^* \qquad (\mathbf{P\Phi}^*)_{rs} = P_{rs}\varphi_s^* \tag{12}$$

where $\varphi_r = \exp(iQd_r)$, d_r is a repeat distance of pure stage r GIC, and $V_{rs} = V_r^* V_s$. In the thermodynamic limit of large N, $I_N(Q)/N$ becomes

$$I(Q) = \lim_{N\to\infty} \frac{I_N(Q)}{N} = \text{Tr}\left\{(\mathbf{FV})\left(\frac{1}{1-\mathbf{P\Phi}}\right)\right\} + \text{Tr}\left\{\mathbf{FV}^*\left(\frac{1}{1-\mathbf{P\Phi}^*}\right)\right\} - \text{Tr}(\mathbf{FV}). \tag{13}$$

2.2. Effect of stage disorder on (00L) x-ray Bragg reflection

For simplicity we consider the x-ray scattering intensity of a system having a stage disorder with $P_{sr} = f_s$, which is described as

$$I(Q) = \sum_r f_r |V_r|^2 + 2\text{Re}\left\{\frac{1}{1-\sum_r \varphi_r f_r}\chi(Q)\right\} \tag{14}$$

for $\sum_r \varphi_r f_r \neq 1$, where $\chi(Q)$ is the structure factor and defined by

$$\chi(Q) = \left[\sum_{s,t} f_s f_t \varphi_s V_t^* V_t\right]. \tag{15}$$

Figure 2 shows a typical example of the calculation on the x-ray scattering intensity of the CoCl$_2$-GIC system along (00Q) where the probabilities f_2 and f_3 are valid as parameters ($f_2 \geqslant f_3$ and $f_2 + f_3 = 1$). The lattice parameter $d_2 = 12.789$ Å, $d_3 = 16.139$ Å
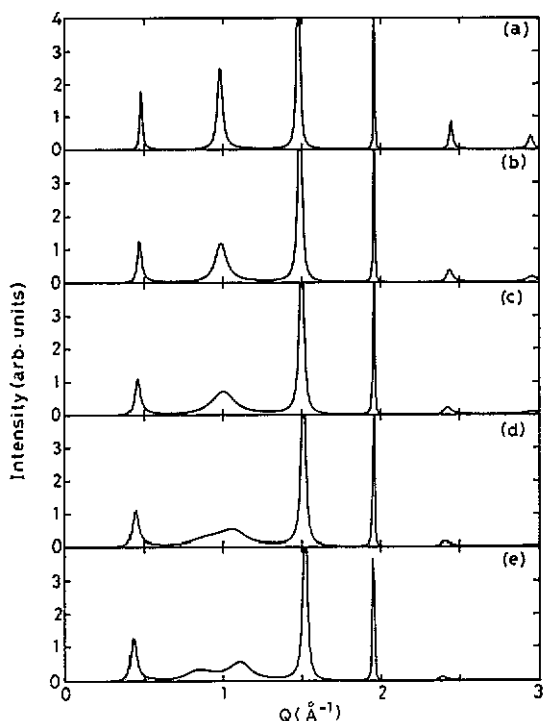
Figure 2. Model calculation of $(00L)$ x-ray diffraction profiles for the $CoCl_2$-GIC system with a stoichiometry of $C_{10.85}CoCl_{2.48}$, where packages of stage 2 (f_2) with $d_2 = 12.789$ Å and stage 3 (f_3) with $d_3 = 16.139$ Å are randomly distributed along the c-axis; $f_2 + f_3 = 1$ and $z_1 = 1.39$ Å. (a) $f_2 = 0.9$, (b) $f_2 = 0.8$, (c) $f_2 = 0.7$, (d) $f_2 = 0.6$, and (e) $f_2 = 0.5$.

and $z_1 = 1.39$ Å are assumed. The stoichiometry of this system ($C_{10.849}CoCl_2$) and the Q-dependence of the structure factor V_r ($r = 1, 2$ and 3) described by (4) are taken into account in this calculation. We find from figure 2 that the peak position of the Bragg reflections shifts slightly from that of pure stage 2 $(f_2 = 1)$ described by $Q = (2\pi/d_2)L$ where L is an integer and the Bragg reflection index of pure stage 2. The peak shift (PS) of the Bragg reflection from that of pure stage 2, in fact, oscillates with index L. We also find that the full-width at half-maximum (FWHM) of the Bragg reflections oscillates with index L. These results indicate that the degree of oscillation of FWHM and PS with L is a measure of the stage disorder. The FWHM at $L = 2$ is larger than that at $L = 4$ even for the case of $f_2 = 0.9$ and $f_3 = 0.1$. The FWHM at $L = 2$ monotonically increases with decreasing f_2, while the FWHM at $L = 4$ remains almost unchanged. For the case of $f_2 = f_3 = 0.5$ the Bragg peak at $L = 2$ splits into two broad peaks. These features are common to the $(00L)$ x-ray diffraction pattern of the $Co_cM_{1-c}Cl_2$-GIC system ($c \neq 0$) because the atomic factors $b_{Mn}(Q)$ and $b_{Ni}(Q)$ are assumed to be almost the same as $b_{Co}(Q)$.

From the above example we find it suitable to assume that the x-ray scattering intensity of the $Co_cM_{1-c}Cl_2$-GIC systems has sharp Bragg peaks around

$$Q_h^{(u)} = 2\pi h/d_u \qquad (h: \text{integer}) \qquad (16)$$

for the system in which f_u is larger than the other f_s($f_u \approx 1$ and $f_s \approx 0$ ($s \neq u$)), where d_u is a repeat distance of pure stage-u GIC. Then the x-ray scattering intensity around $Q_h^{(u)}$ can be written as

$$I(Q) = \sum_r f_r |V_r|^2 + \frac{2}{f_u d_u} \frac{\Gamma(Q) \operatorname{Re}(\chi(Q)) - (Q - Q_h^{(u)} - \Sigma(Q)) \operatorname{Im}(\chi(Q))}{(Q - Q_h^{(u)} - \Sigma(Q))^2 + (\Gamma(Q))^2} \qquad (17)$$

where

$$\Sigma(Q) = -\frac{1}{f_u d_u}\sum_r f_r \sin(Qd_r) + (Q - Q_h^{(u)}) \tag{18}$$

and

$$\Gamma(Q) = \frac{1}{f_u d_u}\sum_r f_r[1 - \cos(Qd_r)]. \tag{19}$$

The stage-disorder induced FWHM and PS can be calculated in the approximation that $\Sigma(Q), \Gamma(Q), \chi(Q)$ and $|V_r|^2$ are expanded around $Q = Q_h^{(u)}$. Noting that $f_u \gg f_r\,(u \neq r)$ and the first term of (17) appears only in the third order approximation, (17) is reduced to a simple Lorentzian form in the first order approximation. Then, the FWHM of the Bragg reflection from $Q_h^{(u)}$ and the PS of the Bragg reflection around $Q_h^{(u)}$ can be described by

$$\Delta_{\text{FWHM}} = 2\Gamma(Q_h^{(u)}) \qquad \text{and} \qquad \Delta_{\text{PS}} = \Sigma(Q_h^{(u)}) \tag{20}$$

which are independent of the structure factors. The higher order corrections of FWHM and PS are also calculated by incorporating the higher order terms of $\Sigma(Q), \Gamma(Q), \chi(Q)$ and $|V_r|^2$ in (17).

Now we consider the case when stage 1, stage 2 and stage 3 packages with the probabilities of f_1, f_2 and f_3 ($f_2 \gg f_1 + f_3$ and $f_1 + f_2 + f_3 = 1$) are randomly arranged along the c-axis. The FWHM and PS to the second-order approximation can be given by

$$\begin{aligned}
\Delta_{\text{FWHM}} = {}& 2[(f_1 + f_3)/f_2 d_2]\{1 - \cos(Q_L^{(2)}c_2)\} - (1/f_2^2 d_2^2)(f_1^2 + f_3^2)d_2 \\
& + (2/f_2^2 d_2^2)(f_1^2 - f_3^2)c_2 \cos(Q_L^{(2)}c_2) + (1/f_2^2 d_2^2)\{(f_1^2 + f_3^2)d_2 \\
& - 2(f_1^2 - f_3^2)c_2\}\cos(2Q_L^{(2)}c_2)
\end{aligned} \tag{21}$$

and

$$\begin{aligned}
\Delta_{\text{PS}} = {}& [(f_1 - f_3)/f_2 d_2]\sin(Q_L^{(2)}c_2) - [(f_1 + f_3)/2f_2^2 d_2^2]\{(f_1 - f_3)d_2 \\
& + (f_1 + f_3)c_2\}\sin(Q_L^{(2)}c_2) + (1/4f_2^2 d_2^2)\{-(f_1^2 - f_3^2)d_2 \\
& + (3f_1^2 + 3f_3^2 - 2f_1 f_3)c_2\}\sin(2Q_L^{(2)}c_2) + U(V_1, V_2, V_3)
\end{aligned} \tag{22}$$

where $Q_L^{(2)} = (2\pi/d_2)L$ (L; integer), and the first terms of (21) and (22) correspond to the first order approximation of the calculations. The PS becomes dependent on the structure factor V_r through a function $U(V_r)$ which is not shown in an explicit form here. The FWHM remains independent of the structure factor V_r.

Here we show that the first order approximation gives a good approximation for the values of the FWHM and PS which are calculated for the following three examples. Figure 3 shows (a) FWHM and (b) PS for the CoCl$_2$-GIC system consisting of packages with stage 1 ($f_1 = 0.2$) and stage 2 ($f_2 = 0.8$), as a function of the Bragg index L of pure stage 2, where the exact values of FWHM and PS are denoted by closed circles. For comparison the values of the FWHM and PS described by the first terms of (21) and (22) are plotted by full curves as a function of $Q_L^{(2)}$ for any L, in spite of the fact that these equations are valid only for integer L. The closed circles are found to be located on the full curves at integer L. Figure 4 shows (a) FWHM and (b) PS for the CoCl$_2$-GIC system consisting of packages with stage 2 ($f_2 = 0.8$) and stage 3 ($f_3 = 0.2$), as a function of the index L of pure stage 2. While the oscillation form of FWHM with L in figure 4(a) is similar to that in figure 3(a), the phase in the oscillation of PS in figure 4(b) is different from that in
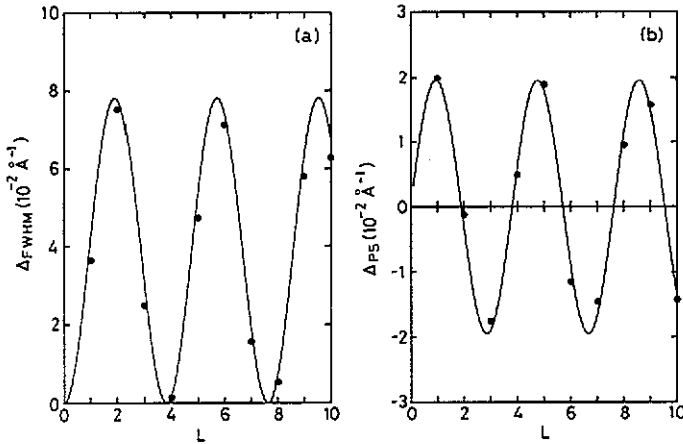
Figure 3. Model calculations of (*a*) FWHM and (*b*) PS for the $CoCl_2$-GIC system with a random mixture of stage 1 (f_1) and stage 2 (f_2), as a function of the Bragg index of stage 2, L: $f_2 = 0.8$ and $f_1 = 0.2$. The exact values of FWHM and PS are denoted by closed circles and the first order approximation is denoted by full curves.

Figure 4. Model calculations of (*a*) FWHM and (*b*) PS for the $CoCl_2$-GIC system with a random mixture of stage 2 (f_2) and stage 3 (f_3), as a function of the Bragg index of stage 2, L: $f_2 = 0.8$ and $f_3 = 0.2$. The exact values of FWHM and PS are denoted by closed circles and the first order approximation is denoted by full curves.
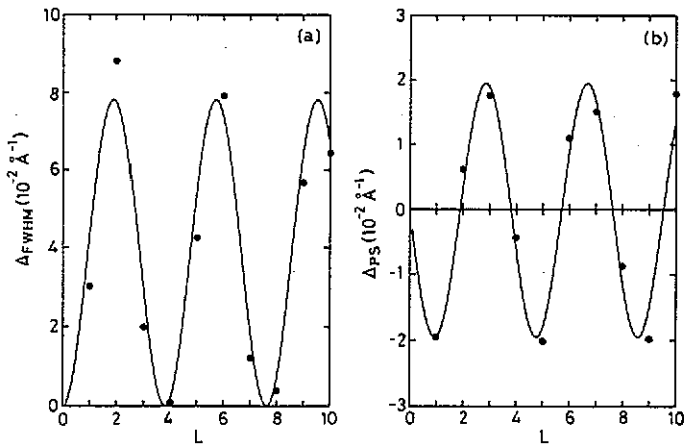
figure 3(*b*) by π. This result can be generalized as follows: the phase of the PS oscillation for the system consisting of majority stage n and minority stage $n - 1$ is different from that for the system consisting of majority stage n and minority stage $n + 1$ by π. In fact, such a phase shift of the PS oscillation has been reported for the stage 7 K-GIC by Fischer *et al* (1983). Figure 5 shows (*a*) FWHM and (*b*) PS for the $CoCl_2$-GIC system consisting of packages with stage 1 ($f_1 = 0.1$), stage 2 ($f_2 = 0.8$) and stage 3 ($f_3 = 0.1$), as a function of the index L of pure stage 2. For $f_1 = f_3$ the PS to the first order approximation is zero, and the oscillation of the PS is obtained in the second order approximation. It is found
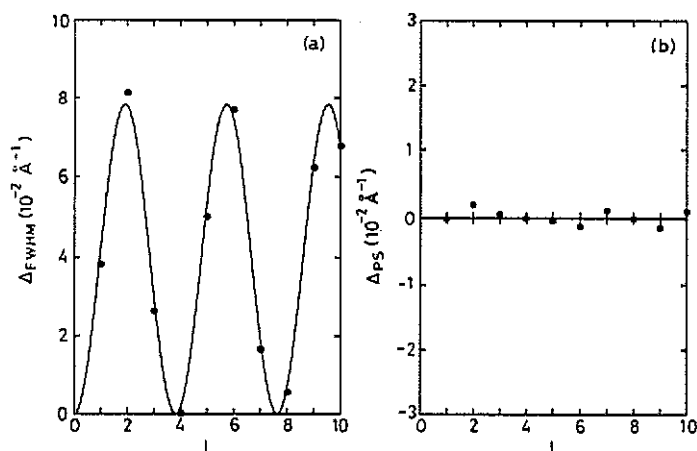
Figure 5. Model calculations of (*a*) FWHM and (*b*) PS for the CoCl$_2$-GIC system with a random mixture of stage 1 (f_1), stage 2 (f_2) and stage 3 (f_3), as a function of the Bragg index of stage 2, L : $f_1 = f_3 = 0.1$ and $f_2 = 0.8$. The exact values of FWHM and PS are denoted by closed circles and the first order approximation is denoted by full curves. Note that the full curve of the PS coincides with the $\Delta_{PS} = 0$ line.

from figures 3, 4 and 5 that the exact values of the FWHM and PS denoted by the closed circles is in good agreement with the full curves described by the first terms of (21) and (22). Thus, it is concluded that the exact values of the FWHM and PS in figures 3, 4 and 5 agree very well with the first order approximations for the case of $f_2 = 0.8$. This result indicates that the oscillation of the FWHM and PS induced by the stage disorder depends only on (i) probability, (ii) c-axis repeat distance and (iii) distance c_2. Since the first order approximation is completely independent of the structure factors, it may be applicable to the analysis of the (00L) x-ray diffraction data of GIC systems having a dominant stage number and stage disorder. As f_2 decreases further ($f_1 + f_2 + f_3 = 1$), the second order approximation gives a better approximation for the exact values of the FWHM and PS.

3. Experimental procedure

The Co$_c$M$_{1-c}$Cl$_2$-GIC (M $\equiv$ Mn, Ni) samples were synthesized by heating a mixture of single crystal Kish graphites (SCKG) and single crystal Co$_c$M$_{1-c}$Cl$_2$ in a chlorine gas atmosphere with a pressure of 740 Torr. The reaction was continued at 773 K for 20 days. After the samples were quenched from 773 K to 300 K, the stage of these samples was examined by (00L) x-ray diffraction. The fraction of stage 2 is found to be much larger than that of the other stages in these compounds. For convenience hereafter 'stage 2' refers to these samples. The characterization of the stage 2 Co$_c$M$_{1-c}$Cl$_2$-GICs (M = Mn, Ni) is listed in table 1. The Co concentration of samples used here was determined from the DC magnetic susceptibility measurements (Yeh *et al* 1990, Suzuki *et al* 1991).

The (00L) x-ray diffraction of the stage 2 Co$_c$Mn$_{1-c}$Cl$_2$-GICs and stage 2 Co$_c$Ni$_{1-c}$Cl$_2$-GICs with $0 \leqslant c \leqslant 1$ was measured at 300 K by using a Huber double circle diffractometer with a MoKα x-ray radiation source (1.5 kW) and a HOPG monochromator. An entrance slit of 2 $\times$ 2 mm^2 was placed between the monochromator and the sample. The x-ray

Table 1. Characterization of stage 2 $Co_cMn_{1-c}Cl_2$-GICS ($\#CM$: $C_nCo_cMn_{1-c}Cl_{2+\delta}$) and stage 2 $Co_cNi_{1-c}Cl_2$-GICS ($\#CN$: $C_nCo_cNi_{1-c}Cl_{2+\delta}$), where d_2 is the c-axis repeat distance, z_1 is the distance between the Cl layer and the Co_cM_{1-c} layer (M = Mn, Ni), and the diameter of islands D_2 is given by (24) with $a_G^2/\Delta = 3.07$.

Sample	c	d_2 (Å)	z_1 (Å)	n	δ	D_2 (Å)
$\#CM00$	0.0	12.893 ± 0.036	1.40	16.28	1.69	51
$\#CM05$	0.05	12.848 ± 0.058	1.40	11.65	0.43	144
$\#CM10$	0.10	12.847 ± 0.027	1.40	15.90	0.64	132
$\#CM20$	0.20	12.878 ± 0.064	1.40	16.69	1.03	86
$\#CM25$	0.25	12.871 ± 0.034	1.40	10.32	0.51	107
$\#CM40$	0.40	12.809 ± 0.036	1.37	11.43	0.51	119
$\#CM50$	0.50	12.833 ± 0.066	—	—	—	—
$\#CM70$	0.70	12.796 ± 0.058	—	—	—	—
$\#CM85$	0.85	12.792 ± 0.036	1.38	11.67	0.41	151
$\#CM90$	0.90	12.787 ± 0.026	1.38	10.84	0.49	117
$\#CM100$	1.00	12.789 ± 0.013	1.39	10.85	0.48	120
$\#CN10$	0.10	12.774 ± 0.440	1.34	13.62	0.89	81
$\#CN19$	0.19	12.766 ± 0.197	1.35	13.70	0.72	101
$\#CN40$	0.40	12.779 ± 0.171	1.40	12.35	0.47	140
$\#CN524$	0.524	12.721 ± 0.352	1.37	14.35	1.26	61
$\#CN63$	0.63	12.766 ± 0.145	1.35	15.26	1.05	77
$\#CN80$	0.80	12.750 ± 0.416	1.39	16.27	1.40	62

beam diffracted by the sample was collimated by the exit slit of 1×1 mm^2 and detected by a Bicron photomultiplier tube.

4. Results

4.1. (00L) x-ray diffraction

The integrated intensity of the (00L) x-ray scattering for our sample of the $Co_cM_{1-c}Cl_2$-GICS (M = Mn, Ni) dominated by the stage 2 fraction is assumed to be the same as that for pure stage 2 described by

$$I(Q) = A|\{2V_C(Q) \cos(Qc_1) + V_1(Q)\}|^2 e^{-B(Q/4\pi)^2} \tag{23}$$

where the exponential factor with a constant B is a Debye–Waller factor. The same type of equation (23) is used by Baron *et al* (1982) to determine the stoichiometry of stage 1 $MnCl_2$-GIC from the (00L) x-ray diffraction data. The numbers of C, Cl, Co and M atoms per unit area which are included in $V_1(Q)$ of (23) are given by $\rho_C = n/2$, $\rho_{Cl} = (2 + \delta)/2$, $\rho_{Co} = c$ and $\rho_M = 1 - c$ for the stoichiometry $C_nCo_cM_{1-c}Cl_{2+\delta}$. Figure 6 shows a typical example of the (00L) x-ray diffraction pattern for $c = 0.4$ ($\#CM40$) with $d_2 = 12.809 \pm 0.036$ Å as a function of Q. We observed sharp Bragg peaks around $Q = (2\pi/d_2)L$ for pure stage 2. The least squares fit of the integrated intensity of Bragg reflections with $L = 1$–12 to (23) yields the values of $z_1 = 1.37$ Å, $n = 11.43$, $\delta = 0.51$ and $B = 11$. By using the same procedure, we determined the values of z_1, n and δ of our stage 2 $Co_cMn_{1-c}Cl_2$-GICS and stage 2 $Co_cNi_{1-c}Cl_2$-GICS with different Co concentrations, these are listed in table 1. Here we assume that the intercalate layer of the $Co_cM_{1-c}Cl_2$-GICS consists of small islands. The excess chlorine atoms on the periphery of islands provide acceptor sites for charges transferred from the graphite layer (Wertheim 1981, Baron *et*
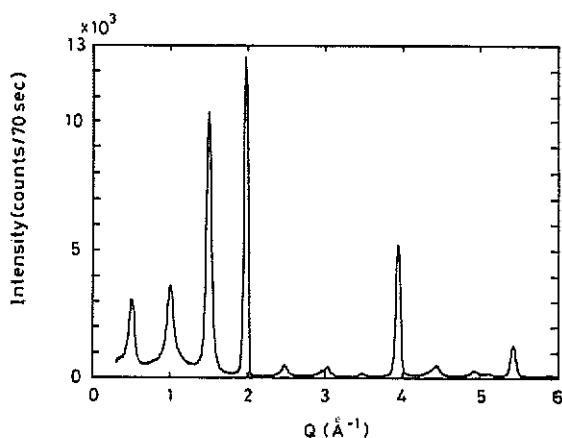
Figure 6. X-ray diffraction pattern of stage 2 $Co_cMn_{1-c}Cl_2$-GIC with $c = 0.40$ ($\#$CM40, $d_2 = 12.809 \pm 0.036$ Å and $z_1 = 1.37$ Å) at 300 K along the $(00Q)$ direction.

al 1982). When the islands are assumed to have the form of a circle, the diameter D_i of the islands for the stage i $Co_cM_{1-c}Cl_2$-GIC having the stoichiometry of $C_nCo_cM_{1-c}Cl_{2+\delta}$ can be estimated as

$$D_2 = 4\sqrt{3}\langle a_2\rangle^2/\Delta\delta = 2\sqrt{3}(a_G^2/\Delta)(n_2/\delta) \qquad (24)$$

with $n_i = n/i$ by using the relation that the ratio of Cl atoms inside the island and on the periphery of the island is equal to $2/\delta$, where $\langle a_i\rangle = (n_i/2)^{1/2} a_G$ is the average in-plane lattice constant inside the island, a_G ($= 2.46$ Å) is the in-plane lattice constant of the graphite layer, and Δ is the distance between nearest neighbour Cl atoms on the periphery. Note that $\langle a_i\rangle$ increases as the intercalate coverage becomes incomplete. The value of (a_G^2/Δ) is estimated as 3.07 by using the results of Baron *et al* (1982): $D_1 = 130$ Å, $\delta = 0.46$ and $n_1 = 5.63$ for the stage 1 $MnCl_2$-GIC. The island diameter can be calculated by using the relation $D_2 = 5.32$ (n/δ) for the stage 2 $Co_cMn_{1-c}Cl_2$-GICs and stage 2 $Co_cNi_{1-c}Cl_2$-GICs (table 1).

4.2. Stage disorder-induced FWHM and PS

The FWHM and peak position of each Bragg peak ($L = 1, 2, \ldots, 12$) was determined from the least squares fit of the $(00L)$ x-ray intensity data of the stage 2 $Co_cMn_{1-c}Cl_2$-GICs and stage 2 $Co_cNi_{1-c}Cl_2$-GICs to the theoretical curve expressed by a sum of Gaussian distribution and quadratic background. Note that this FWHM is not an intrinsic FWHM which can be obtained from a deconvolution of the measured x-ray intensity with the instrumental resolution function. Figure 7(a) shows the L-dependence of the FWHM at 300 K for the stage 2 $Co_cMn_{1-c}Cl_2$-GIC with $c = 0, 0.10, 0.40, 0.50, 0.85$ and 1, where L is the Bragg index of pure stage 2. Most of the FWHMs clearly show local minima at $L = 4$ and 8, and local maxima at $L = 2$ and 6. These results can be explained well in terms of the first term of (21). In fact it shows local minima at $L = 4, 8$, and 12, and local maxima at $L = 2, 6$, and 10 for $c_2 = 3.35$ Å and the value of d_2 listed in table 1. We also find that (i) the height of the local maxima is strongly sample dependent, and that (ii) the height of the local maximum at $L = 2$ is lower than those at $L = 6$ and 10. The latter result seems to be inconsistent with our prediction that the maximum value ξ is
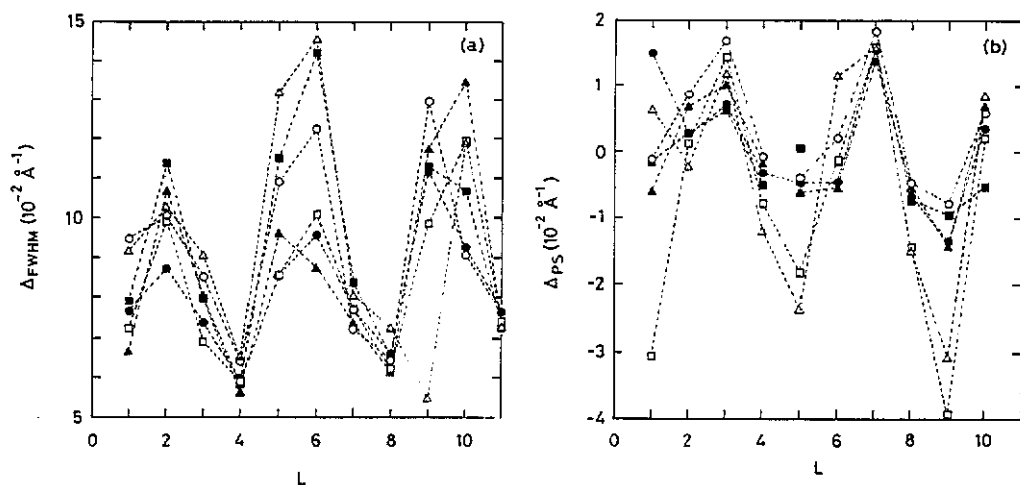
Figure 7. (*a*) *L*-dependence of FWHM at 300 K for the stage 2 $Co_cMn_{1-c}Cl_2$-GICs with $c = 0$ (O), 0.10 (▲), 0.40 (●), 0.50 (△), 0.85 (■) and 1 (□), where *L* is the Bragg index of pure stage 2. (*b*) *L*-dependence of PS at 300 K for the stage 2 $Co_cMn_{1-c}Cl_2$-GICs with $c = 0$ (O), 0.05 (▲), 0.10 (●), 0.20 (△), 0.40 (■) and 0.70 (□) where *L* is the Bragg index of stage 2.

Table 2. Fractional probability of stage number in stage 2 $Co_cMn_{1-c}Cl_2$-GICs (#CM) and stage 2 $Co_cNi_{1-c}Cl_2$-GICs (#CN), where f_1, f_2 and f_3 are the probability of finding stage 1, 2 and 3, respectively, in samples.

Sample	c	$f_1 (\%)$	$f_2 (\%)$	$f_3 (\%)$
#CM00	0.0	0	86.0	14.0
#CM05	0.05	0	91.0	9.0
#CM10	0.10	3.2	85.7	11.1
#CM20	0.20	3.3	81.1	15.6
#CM25	0.25	7.6	91.5	0.9
#CM40	0.40	1.0	90.7	8.3
#CM50	0.50	1.5	86.7	11.8
#CM70	0.70	3.5	78.6	17.9
#CM85	0.85	4.9	84.3	10.8
#CM90	0.90	2.6	88.2	9.2
#CM100	1.00	12.5	87.5	0
#CN10	0.10	5	76	19
#CN19	0.19	0	84	16
#CN40	0.40	20	56	24
#CN524	0.524	—	—	—
#CN63	0.63	17	57	26
#CN80	0.40	5	61	34

independent of L: $\xi = 4(1 - f_2)/f_2 d_2$. The value ξ is expected to increase with decreasing f_2. When a typical value of the intrinsic FWHM is assumed to correspond to the observed FWHM at $L = 2$ minus a minimum value of the FWHM ($\approx 0.055 \text{ Å}^{-1}$), then the fractional probability f_2 in each sample can be estimated by comparing the peak value of the intrinsic FWHM with the value ξ (table 2).
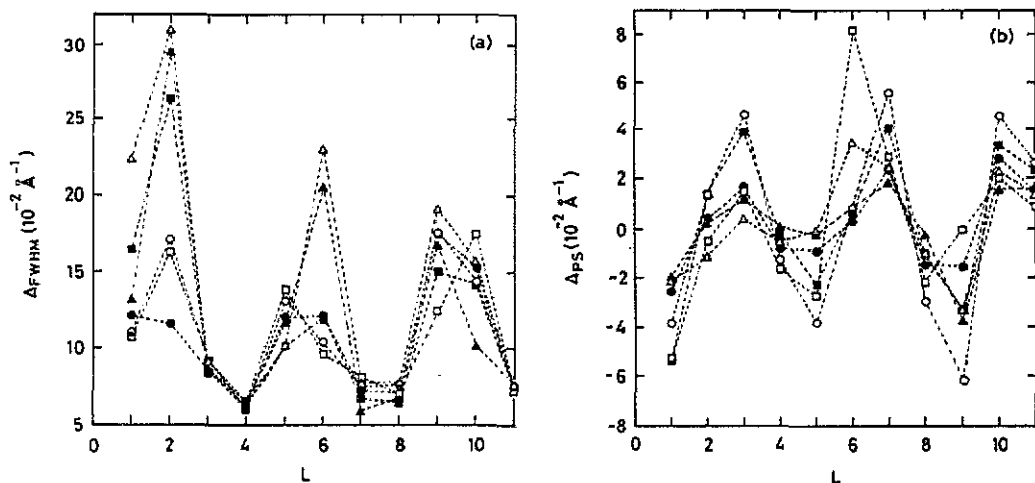
Figure 8. L-dependence of (*a*) FWHM and (*b*) PS at 300 K for the stage 2 $Co_cNi_{1-c}Cl_2$-GICs with $c = 0.10$ ($\square$), 0.19 ($\bullet$), 0.40 ($\triangle$), 0.524 ($\bigcirc$), 0.63 ($\blacktriangle$) and 0.80 ($\blacksquare$), where L is the Bragg index of stage 2.

Figure 7(*b*) shows the L-dependence of the PS of the $(00L)$ Bragg reflection from the average position $Q = (2\pi/d_2) L$ for the stage 2 $Co_cMn_{1-c}Cl_2$-GICs with $c = 0, 0.05$, $0.10, 0.20, 0.40$, and 0.70. The PS has local minima at $L = 5$ and 9, and local maxima at $L = 3$ and 7. This periodicity can be explained well by the first term of (22). The phase of the PS oscillation indicates that these compounds consist of majority stage 2 and minority stage 3. Although the PS oscillation for $c = 0.25$ and 1 is not shown in figure 7(*b*), the phase of the PS oscillation for $c = 0.25$ and 1 is different from that shown in figure 7(*b*) by π, indicating that the samples with $c = 0.25$ and 1 consist of majority stage 2 and minority stage 1. When we assume that the peak value at $L = 3$ can be expressed by $\zeta = (f_1 - f_3)/f_2 d_2$, we can calculate the values of f_1 and f_3 for each sample (table 2) by using the value of f_2 obtained from the FWHM.

Figure 8(*a*) shows the L-dependence of the FWHM at 300 K for the stage 2 $Co_cNi_{1-c}Cl_2$-GICs with $c = 0.10, 0.19, 0.40, 0.524, 0.63$, and 0.80, where L is the Bragg index of stage 2. The FWHM shows local minima at $L = 4$ and 8, and local maxima at $L = 2$ and 6. The peak value of the local maxima at $L = 2$ is strongly sample dependent. When a typical value of the intrinsic FWHM is assumed to correspond to the observed FWHM at $L = 2$ minus a minimum value of the FWHM (≈ 0.061 Å^{-1}), then the fractional probability f_2 in each sample can be estimated by comparing the peak value of intrinsic FWHM with the value ξ (table 2).

Figure 8(*b*) shows the L-dependence of the peak shift (PS) of the $(00L)$ Bragg reflection from the average position $Q = (2\pi/d_2) L$, for the stage 2 $Co_cNi_{1-c}Cl_2$-GICs with $c = 0.1, 0.19, 0.40, 0.524, 0.63$, and 0.80, where L is the Bragg index of stage 2. The PS in figure 8(*b*) shows local maxima at $L = 3$ and 7, and local minima at $L = 5$ and 9, indicating that fractional probability f_3 is larger than f_1 for the samples with $c = 0, 0.1$, $0.4, 0.7$ and 0.85. When we assume that the peak value at $L = 3$ can be expressed by ζ, we can calculate the values of f_1 and f_3 for each sample (table 2) by using the value of f_2 obtained from the FWHM. The noticeable feature is that the degree of stage disorder in stage 2 $Co_cNi_{1-c}Cl_2$-GICs is much higher than that in the stage 2 $Co_cMn_{1-c}Cl_2$-GICs.

5. Discussion

As described in section 1, Kirczenow (1985) has proposed the scaling law that the fractional probability f_i of stage-i units is approximated by the Gaussian distribution with centre $\langle i \rangle$ and width $\sigma_{\langle i \rangle}$ given by (1), when f_i is a smoothly varying function of stage i so that i can be regarded as a continuous variable. This scaling law may provide a novel method for determining the interlayer repulsion energy u_i $(= v_0 i^{-\alpha})$ which plays an important role in the stage order. Here we estimate the order of magnitude of v_0 and α for the stage 2 $Co_c Mn_{1-c}Cl_2$-GICS and stage 2 $Co_c Ni_{1-c}Cl_2$-GICS by applying the scaling law to the experimental results on the fractional probability f_1, f_2 and f_3. To this end we may rewrite the normalized fractional probability as a scaling function of μ/v_0

$$f_i/\langle f_i \rangle = \exp\{-[\mu/v_0 - (\alpha + 1)/\langle i \rangle^\alpha]^2/2\sigma^2_{\langle \mu_i \rangle}\} \tag{25}$$

with the width

$$\sigma^2_{\langle \mu_i \rangle} = k_B T \alpha(\alpha + 1)/(N_0 v_0 \langle i \rangle^\alpha). \tag{26}$$

Here the chemical potential μ is measured relative to the in-plane interaction energy corresponding to $\omega = (-\varepsilon z/2) + \gamma$ in the theory of Kirczenow (1985), and is related to the stage i by the approximation

$$\mu - \langle \mu_i \rangle = -x\langle i \rangle[(\partial^2 u_i/\partial i^2)_{i=\langle i \rangle}](i - \langle i \rangle) \tag{27}$$

and $\langle \mu_i \rangle$ is given by

$$\langle \mu_i \rangle = [u_i - (\partial u_i/\partial i)i]_{i=\langle i \rangle} = v_0(\alpha + 1)\langle i \rangle^{-\alpha}. \tag{28}$$

It may be derived from the form of (25) that the fractional probability f_i is described by a scaling function Ψ of μ/v_0

$$f_i/\langle f_i \rangle = \Psi(\mu/v_0; \lambda, \alpha, \langle i \rangle) \tag{29}$$

with

$$\sum_i f_i = 1 \tag{30}$$

for any μ, where λ $(= k_B T/N_0 v_0)$ is a scaling factor, and the scaling function Ψ is the Gaussian distribution function in the immediate vicinity of $\mu = \langle \mu_i \rangle$. The scaling function has a peak at $\mu/v_0 = (\alpha + 1)/\langle i \rangle^\alpha$ for stage i. The width of the peak is determined by the scaling factor λ, and increases as temperature increases and as N_0 and v_0 decrease. The numerical calculations of f_i versus μ have been made by Kirczenow (1985) with α, T, N_0 and v_0 varied as parameters. By using the scaling relation of (29) these numerical calculations can be classified by the value of λ: (i) f_i in figures 1(a) and (b), figures 2(a), (b), (c), (d) and figure 4 of his paper (Kirczenow 1985) corresponds to (29) with $\alpha = 1$ for $\lambda = 3.33 \times 10^{-4}, 5.0 \times 10^{-5}, 1.67 \times 10^{-3}, 5.56 \times 10^{-3}, 5.56 \times 10^{-2}, 5.56 \times 10^{-1}$, and 1.33×10^{-3}, respectively, and (ii) f_i in figures 3(a) and (b) of his paper (Kirczenow 1985) corresponds to (29) with $\alpha = 4$ for $\lambda = 3.33 \times 10^{-4}$ and 3.33×10^{-6}.

Here we make use of these figures with $\alpha = 1$ to estimate the order of v_0 for our compounds consisting of majority stage 2 and minority stage 1 and stage 3. The shift in the peak position of stage 1 $(\mu/v_0 = \alpha + 1)$ to the small side of the μ/v_0-axis becomes larger than that of stage 2 $(\mu/v_0 = (\alpha + 1)/2^\alpha)$ as α decreases, indicating that the probability of overlapping in stage 1 and stage 2 becomes large for small α. Thus, our

choice of $\alpha = 1$ is consistent with the experimental results that f_1 is relatively smaller than that of f_2 but is not negligibly small (table 2). The temperature chosen here corresponds to that of the sample preparation: $T = 773$ K ($k_B T = 0.07$ eV). The number N_0 is determined from the relation $N_0 = (2\pi/4\sqrt{3})(D_2/a)^2$ with a typical value of D_2 ($= 100$ Å) and the in-plane lattice constant $a = 3.56$ Å of stage 2 $CoCl_2$-GIC: $N_0 = 700$. Then the value of λ is calculated as $\lambda = k_B T/N_0 v_0 = 1.0 \times 10^{-4}/v_0$ where v_0 is measured in units of eV.

As is seen from figures 1, 2 and 4 of the Kirczenow's paper (Kirczenow 1985), the degree of stage disorder increases with increasing λ. For λ lower than 1.67×10^{-3} (figures $1(a)$, (b) and $2(a)$), both the transitions between stage 1 and 2, and between stage 2 and stage 3 occur within very narrow ranges of μ/v_0: $f_1 = 1$ at $\mu/v_0 = 2$, $f_2 = 1$ at $\mu/v_0 = 1$, and $f_3 = 1$ at $\mu/v_0 = 2/3$. For $\lambda = 5.56 \times 10^{-3}$ (figure $2(b)$), the transition between stage 2 and stage 3 becomes broader. There still exists a wide region of pure stage 2: $f_1 = 1$ at $\mu/v_0 = 2$, $f_2 = 1$ at $\mu/v_0 = 1$, and $f_3 = 0.99$ and $f_4 = 0.01$ at $\mu/v_0 = 2/3$. For $\lambda = 5.56 \times 10^{-2}$ (figure $2(c)$), the region of pure stage 2 disappears. The regions of stage 1, stage 3 and stage 4 are superimposed on the region of stage 2: $f_1 = 1$ at $\mu/v_0 = 2$, $f_1 = 0.43$, $f_2 = 0.53$, and $f_3 = 0.04$ at $\mu/v_0 = 1$, and $f_1 = 0.07$, $f_2 = 0.57$, $f_3 = 0.28$, and $f_4 = 0.08$ at $\mu/v_0 = 2/3$. Note that the fractional probability of figure $2(c)$ seems not to be described by a scaling function of μ/v_0.

We observe two types of the fractional probability for the stage 2 $Co_c Mn_{1-c} Cl_2$-GICs: (i) $f_2 \gg f_3 > f_1$ (typically, $f_2 = 0.843$, $f_3 = 0.108$, and $f_1 = 0.049$ for #CM85), and $f_2 \gg f_1 > f_3$ (typically, $f_2 = 0.915$, $f_1 = 0.076$, and $f_3 = 0.009$ for #CM25). We also find a little different type of fractional probability for the stage 2 $Co_c Ni_{1-c} Cl_2$-GICs, $f_2 > f_3 > f_1$ (typically, $f_2 = 0.57$, $f_3 = 0.26$, and $f_1 = 0.17$ for #CN63). We assume that (i) these experimental values of fractional probability coincide with the theoretical values at $\mu/v_0 = 1$ for pure stage 2, and that (ii) the value of f_2 at $\mu/v_0 = 1$ decreases monotonically from $f_2 = 1$ to 0.57 as the value of λ changes from $\lambda = 5.56 \times 10^{-2}$ to 5.56×10^{-3} in spite of the lack in numerical calculations of fractional probability for $5.56 \times 10^{-3} < \lambda < 5.56 \times 10^{-2}$. Then there may exist the relation $5.56 \times 10^{-3} < \lambda(Co-Mn) < \lambda(Co-Ni) < 5.56 \times 10^{-2}$, which is rewritten as 1.8×10^{-3} eV $< v_0(Co-Ni) < v_0(Co-Mn) < 1.8 \times 10^{-2}$ eV by using the relation $\lambda = 1.0 \times 10^{-4}/v_0$. Here $\lambda(Co-Mn)$ and $\lambda(Co-Ni)$ are the values of λ, and $v_0(Co-Mn)$ and $v_0(Co-Ni)$ the values of v_0 for the stage 2 $Co_c Mn_{1-c} Cl_2$-GICs and stage 2 $Co_c Ni_{1-c} Cl_2$-GICs. The values of $v_0(Co-Mn)$ and $v_0(Co-Ni)$ are much smaller than that of donor GICs ($v_0 = 0.3$ eV for K-GIC) (Nishitani *et al* 1983), indicating that the charge transfer of our compounds is much smaller than that of K-GIC. The range of μ for the stability of stage 2 and stage 3 can be calculated as $\Delta\mu(2) = 2v_0/3$, and $\Delta\mu(3) = 3v_0/12$, respectively, from the thermodynamic potential at zero temperature (Safran 1988). For our systems these ranges are extremely narrow because of the small value of v_0. The vapour pressure of the intercalant at the stage transition from stage 1 to 2 (P_A) is almost that same as that at the stage transition from stage 2 to 3 (P_B) since $\Delta\mu(2) = k_B T \ln(P_A/P_B)$. This situation makes it difficult to obtain pure stage 2 for our compounds.

6. Conclusion

We have developed a simple method to determine the fractional probability from the stage-disorder induced peak shift and the full-width at half-maximum of the Bragg reflection in the (00L) x-ray diffraction pattern. This method is applicable to donor

GICs as well as acceptor GICs. The fractional probability for each stage in the stage 2 $Co_cMn_{1-c}Cl_2$-GICs and stage 2 $Co_cNi_{1-c}Cl_2$-GICs has been determined by using this method. We have discussed the degree of stage disorder in these compounds on the basis of the scaling hypothesis that the fractional probability for each stage is described by a scaling function of μ/v_0 with a scaling factor $\lambda = k_B T/N_0 v_0$. Note that this scaling hypothesis is theoretically proved to be valid for small λ and high stage number. We have estimated the form of the interlayer repulsion interaction as $u_i = v_0 i^{-\alpha}$ with $\alpha \approx 1$ and $v_0 = 1.8 \times 10^{-3}$–1.8×10^{-2} eV by assuming the scaling hypothesis. The degree of stage disorder in these compounds occurs because of small charge transfer as well as small island size. In these compounds the elastic interaction may be also responsible for the stage order.

Acknowledgments

References

Baron F, Flandrois S, Hauw C and Gaultier J 1982 *Solid State Commun.* **42** 759–62
Cajipe V B, Heiney P A and Fischer J E 1989 *Phys. Rev.* B **39** 4374–85
Fischer J E, Fuerst C D and Woo K C 1983 *Synth. Met.* **7** 1–12
Fuerst C D, Koch T C, Fischer J E, Axe J D, Hastings J B and McWhan D B 1983 *Intercalated Graphites* ed M S Dresselhaus, G Dresselhaus, J E Fischer and M S Moran (New York: North-Holland) pp 39–42
Hendricks S and Teller E 1942 *J. Chem. Phys.* **10** 147–67
Hohlwein D and Metz W 1974 *Z. Kristallogr.* **139** 279–96
Huster M E, Heiney P A, Cajipe V B and Fischer J E 1987 *Phys. Rev.* B **35** 3311–26
Kakinoki J and Komura Y 1952 *J. Phys. Soc. Japan* **7** 30–5
Kim H J, Fischer J E, McWhan D B and Axe J D 1986 *Phys. Rev.* B **33** 1329–39
Kirczenow G 1985 *Phys. Rev.* B **31** 5376–86
—— 1990 *Graphite Intercalation Compounds I* ed H Zabel and S A Solin (New York: Springer) pp 59–100
Metz W and Hohlwein D 1975 *Carbon* **13** 87–96
Misenheimer M E and Zabel H 1985 *Phys. Rev. Lett.* **54** 2521–4
Nishitani R, Uno Y and Suematsu H 1983 *Phys. Rev.* B **27** 6572–5
Safran S A 1988 *Solid State Physics* vol 40 (New York: Academic) pp 183–246
Suzuki I S, Suzuki M, Tien L F and Burr C R 1991 *Phys. Rev.* B **43** 6393–404
Wertheim G K 1981 *Solid State Commun.* **38** 633–5
Yeh M, Suzuki I S, Suzuki M and Burr C R 1990 *J. Phys.: Condens. Matter* **2** 9821–36